J. Phys. Chem. A **2000,** *104,* 11891−11896

Vibrational Spectroscopy for Size-Selected Fluorene−$(H_2O)_{n=1,2}$ Clusters in Supersonic Jets

Nikhil Guchhait, Takayuki Ebata,* and Naohiko Mikami*

Department of Chemistry, Graduate School of Science, Tohoku University, Sendai 980-8578, Japan

Received: August 15, 2000; In Final Form: September 26, 2000

The OH and CH stretching vibrations of fluorene−$(H_2O)_{n=1,2}$ clusters have been observed by IR−UV and stimulated Raman−UV double resonance spectroscopy in supersonic jets. For fluorene−$(H_2O)_1$, a clear intensity alternation was observed for the symmetric and antisymmetric OH stretching modes in the IR and the Raman spectra, while in fluorene−$(H_2O)_2$ the IR spectrum of the OH stretching vibration indicates the water dimer formation in the cluster. For the CH stretching vibration it was found that the aliphatic CH stretching vibration shows a remarkable blue shift in the clusters. From the observed spectra and the ab initio calculations at HF/6-31G and HF/6-31G(d,p) levels, it was concluded that the $n = 1$ and 2 clusters have similar structures in which the water monomer or the dimer locates above the plane of fluorene.

Introduction

Spectroscopic studies on water-containing clusters are fascinating in the investigation of the hydrogen-bonding property of water. Many properties of water are thought to arise from its special ability to form the networks of hydrogen bonds, where a water molecule behaves both as a hydrogen donor and as an acceptor. The investigations on pure water clusters have been extensively performed both theoretically and experimentally to provide us with the information of structures, energetics, and dynamics of the networks in the clusters.[1−6] Another interesting system is the hydrated clusters of aromatic molecules, which are thought to be a microsolution of aromatic molecules in aqueous solution.[7−9] A number of spectroscopic methods have been applied, such as electronic,[10−13] microwave,[14,15] IR,[16−26] Raman,[27−29] rotational-resolved laser-induced fluorescence,[30−32] and stimulated emission pumping[33] spectroscopies to obtain the information on the structures and dynamics of the clusters. Among those, the double-resonant vibrational spectroscopy has been demonstrated to be a promising method to determine the structures of hydrogen-bonded clusters.[16−29] Our group performed IR−UV double-resonance experiments for the hydrogen-bonded clusters of aromatic molecules having an OH group and reported that the alcoholic OH group is involved in the large hydrogen bond network of water molecules.[17−19,21] Zwier's group applied IR−UV double-resonance spectroscopy to benzene−water clusters and characterized the single, double, π-hydrogen-bonded OH stretching vibrations, which allows them to interpret the probable water clusters' structure.[34,35] It was found that, in all the clusters, water clusters are bound to the benzene ring with a weak π-hydrogen bond. For substituted benzene, such as fluorobenzene[36] or benzonitrile,[28,37] on the other hand, recent experiments and theoretical calculations showed that water molecules are bound on the side of the benzene ring.

In this paper, we present the vibrational spectroscopic study of the fluorene−water clusters prepared in supersonic jets. It is known that most aromatic hydrocarbons exhibit a drastic increase in its acidity in the first electronic excited state and some of them induce proton-transfer reactions with solvent molecules. Fluorene is one of the molecules whose acidity largely changes in S_1 (pK_a = −8.6) compared to S_0 (pK_a = 20.5).[38] For the fluorene−water clusters in jets, Bernstein's group performed mass-resolved multiphoton ionization and dispersed emission spectroscopic studies.[39] They proposed the most probable structures of the clusters and concluded very little chance of proton transfer in the excited state. The purpose of the present work is to determine the structure of fluorene−water clusters by examining the OH stretching mode of the water site as well as CH stretching vibrations of the fluorene site with IR−UV and stimulated Raman−UV double-resonance spectroscopies. With the aid of ab initio calculations, the clusters structures in the ground state are discussed.

Experimental Section

The details of the experimental setup were described in our earlier publication.[17,21,28] The jet-cooled molecules were generated by pulsed supersonic expansion of a gaseous mixture of helium with fluorene (heated at 330 K) and water. IR and Raman spectra of the clusters were obtained as fluorescence-dip spectra, so-called fluorescence detected infrared (FDIR) and fluorescence detected stimulated Raman (FDSR) spectra. In these spectroscopies, the jet-cooled molecules or clusters were monitored by laser-induced fluorescence (LIF) with a pulsed UV laser light. The fluorescence signal was used as a measure of the ground-state population. For the measurement of the FDIR spectrum, a tunable pulsed IR laser light was introduced at 50 ns prior to the UV pulse and its frequency was scanned. When the IR frequency is resonant to the vibrational transition, the ground-state population is reduced, resulting in a depletion of the fluorescence signal. Thus, fluorescence-dip spectra were obtained by scanning the IR wavelength while monitoring the fluorescence signal.

For the measurement of FDSR spectra, the same laser system was used. Two laser lights, a second harmonic of the Nd:YAG laser (ν_1) and a Nd:YAG laser pumped dye laser (ν_2), were used for the stimulated Raman pumping. They were combined by a beam combiner and coaxially introduced into the chamber in a counterpropagated manner to the UV light. The Raman spectrum was observed by scanning the ν_2 laser frequency while monitoring the fluorescence signal. When the difference frequency, $\nu_1 - \nu_2$, was resonant to the vibrational transition, a depletion was observed in the fluorescence signal.

10.1021/jp002958m CCC: $19.00 © 2000 American Chemical Society
Published on Web 11/30/2000

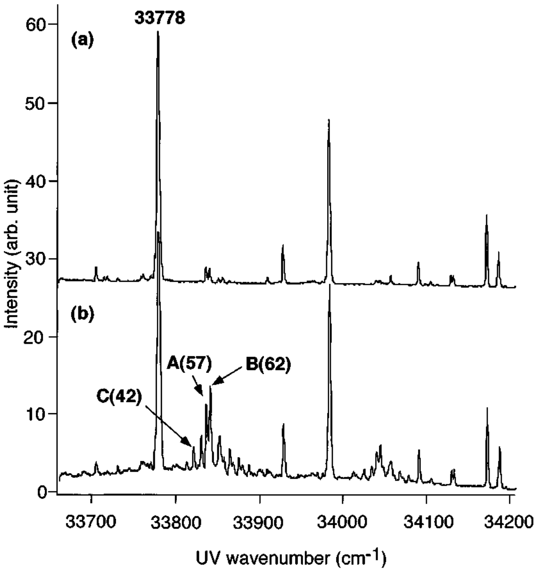

Figure 1. LIF excitation spectrum of jet-cooled fluorene and its clusters with water in the band origin region of the S_1-S_0 transition. The spectrum was measured (a) at low water vapor pressure and (b) at higher water vapor pressure.

The UV light was a second harmonic of a XeCl excimer laser pumped dye laser (Lambda Physik LPX 100/FL 2002). The IR beam was generated with a $LiNbO_3$ crystal by a difference frequency mixing between a part of the second harmonic of an injection seeded Nd:YAG laser (Quanta Ray GCR 230) and the output of the Nd:YAG laser pumped dye laser (Continuum: ND-6000). The same Nd:YAG laser/dye laser system was used for the stimulated Raman pumping. The fluorescence was collected by lenses and detected by a photomultiplier tube (Hamamatsu photonics 1P28). The output signal was processed by a boxcar integrator (PAR 4420) connected to a personal computer.

Ab initio molecular orbital calculations for equilibrium conformers of fluorene$-(H_2O)_n$ clusters were performed with the Gaussian 94 program at HF/6-31G and HF/6-31G(d,p) levels. Full energy optimized structures were calculated without any geometry constraints. Obtained vibrational frequencies were multiplied by a scaling factor of 0.906 at the HF/6-31G level and 0.874 at the HF/6-31G(d,p). The scaling factors were determined from a least-squares fitting of the calculated IR spectra of the most probable structures to those of the observed ones. Fluorene was purchased from Aldrich Chemical Co. and was used without further purification.

Results and Discussions

1. Fluorene$-$H$_2$O. Figure 1a shows the laser-induced fluorescence excitation (LIF) spectrum of fluorene in a jet, being measured under a low concentration of water vapor. The strongest band at 33 778 cm^{-1} and all other bands belonging to the monomer are in good agreement with the reported spectra.[39−41] Figure 1b shows the LIF spectrum obtained under a higher water vapor pressure for the jet expansion. It is seen that the bands belonging to fluorene$-(H_2O)_n$ increase their intensities. As seen in the figure, the S_1-S_0 transitions of the fluorene$-(H_2O)_n$ clusters are blue shifted from the monomer band and are very congested, which also reproduced well with the earlier work.[39] The origin (band A) of the S_1-S_0 transition of fluorene$-H_2O$ appears at the 57 cm^{-1} higher frequency side of the monomer origin and that of fluorene$-(H_2O)_2$ locates at the 42 cm^{-1} (band C) higher frequency side. For the band at 62 cm^{-1} (band B), Bernstein's group interpreted that two transitions due to fluorene$-H_2O$ and $-(H_2O)_2$ are overlapped in this band.[39] They also emphasized that progressions of intermolecular modes due to different sizes of the clusters occur closely with each other, which make the LIF spectrum complicated. The high-frequency shifts of the electronic transitions and an intense progression of the intermolecular mode indicate a decrease of the stabilization energy and a large geometric change of the clusters in S_1. Interestingly, the decrease of the stabilization energy of the clusters in S_1 presents a contradicted result against a reported increase of acidity of fluorene in S_1 in the condensed phase.[38]

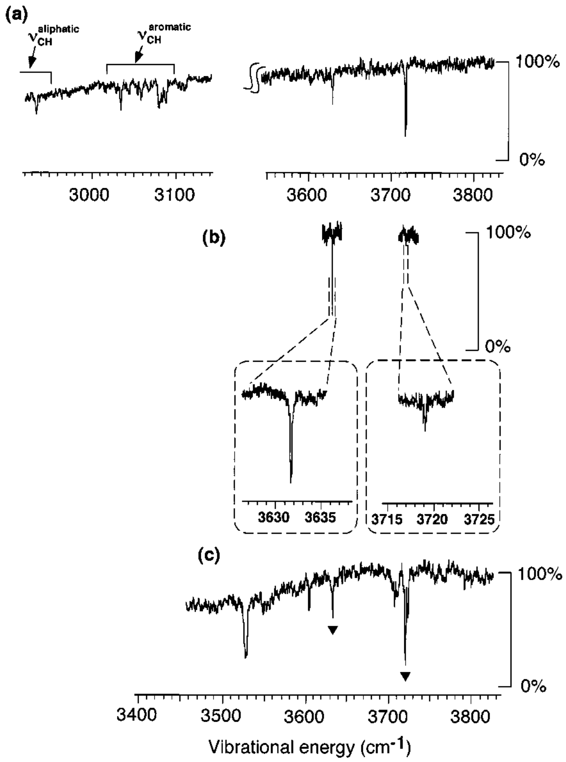

Figure 2. (a) Fluorescence-detected infrared (FDIR) and (b) fluorescence-detected stimulated Raman (FDSR) spectra of fluorene$-H_2O$ obtained by fixing the UV laser frequency to band A in Figure 1. (c) FDIR spectrum obtained by monitoring band B of Figure 1.

Figure 2a shows the FDIR spectrum of fluorene$-H_2O$ obtained by tuning the UV laser frequency to band A. The spectrum shows two OH stretching bands at 3719 and 3632 cm^{-1} of the H_2O site, which are listed in Table 1. As seen in Figure 2a, the dip intensity of the former band is stronger than that of the latter band. The aromatic and aliphatic CH stretching bands are seen in the 2900$-$3100 cm^{-1} region. Figure 2b shows the FDSR spectrum of fluorene$-H_2O$ in which the UV frequency is also fixed to band A. It is seen that the intensity of the 3632 cm^{-1} band is much stronger than that of the 3719 cm^{-1} band. The intensity alternation for the two OH stretch bands between the IR and Raman spectra leads to a conclusion that the bands at 3719 and 3632 cm^{-1} correspond to the antisymmetric and the symmetric modes, respectively. This intensity alternation is very similar to that of free H_2O, and the result indicates that two OH oscillators of H_2O in fluorene$-H_2O$ must be symmetrically equivalent. Another noticeable point is that the antisymmetric and symmetric modes of H_2O exhibit a red shift of 37 and 19 cm^{-1}, respectively, from those of free water.[42] The magnitudes of the shifts are smaller than those of the σ-type hydrogen bond,[17] which is more than 100 cm^{-1}, and close to that of the π-type hydrogen bond.[21,34,35] Thus, such

TABLE 1: Observed and Calculated OH Stretching Vibrational Frequencies (cm^{-1}) for Energy-Optimized Minimum Energy Conformer of Fluorene−Water Clusters

observed frequency	assignment[a]	relative intensity[b] IR	Raman	calculated frequency[c]
		(1:1) Water Cluster		
2927	$\nu_{CH}^{aliphatic}$	w		
3027	$\nu_{CH}^{aromatic}$	vw		
3052	$\nu_{CH}^{aromatic}$	w		
3072	$\nu_{CH}^{aromatic}$	w		
3081	$\nu_{CH}^{aromatic}$	w		
3632	ν_1	m	s	3623(20/38)[d]
3719	ν_3	s	w	3719(45/21)[d]
		(1:2) Water Cluster		
3527	ν_1	vs	m	3554(168/82)[e]
3604	ν_1	s	m	3610(64/32)[e]
3706	ν_3	m		3696(95/81)[e]
3710		m		
3722	ν_3	s	vw	3722(55/25)[e]

[a] ν_3: antisymmetric OH stretching mode. ν_1: symmetric OH stretching mode. [b] Intensity: vs, very strong; s, strong; m, medium; w, weak; vw, very weak. [c] All values are rounded up to the nearest number. Values are taken from the HF/6-31G(d,p) level calculation and are multiplied by a factor of 0.874. Numbers in the parentheses are calculated IR intensity (km/mol) and Raman activity (Å^4 amu^{-1}), respectively. [d] Conformer I of Figure 3. [e] Conformer I of Figure 8.

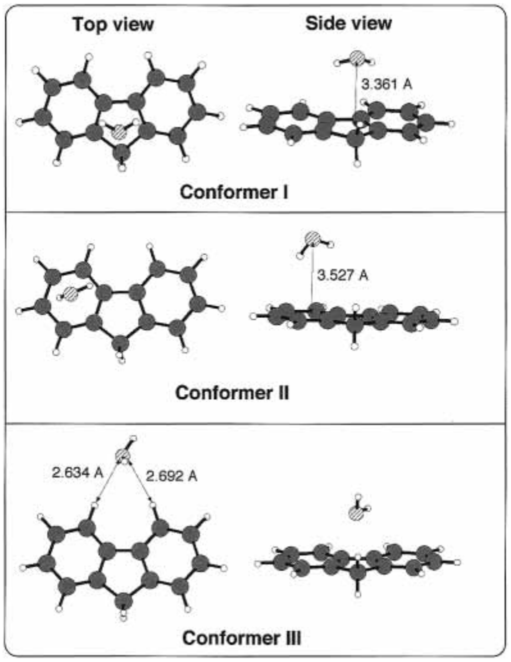

Figure 3. For conformers I and II, the distance of an oxygen atom of H_2O from the plane of fluorene is indicated. Energy-optimized structures of fluorene−H_2O obtained at the HF/6-31G(d,p) level calculation.

small red shifts for both modes suggests that H_2O is bound to the π-electron of fluorene.

Figure 2c shows the FDIR spectrum obtained by fixing the UV frequency to band B. In the spectrum of band B, a number of bands appear at the OH stretching region. It is seen, however, that the two bands at 3719 and 3632 cm^{-1} coincide with the vibrations observed by monitoring band A. In addition, it was found that other bands are due to the OH stretching vibrations of fluorene−$(H_2O)_2$ from the comparison of the spectrum with the FDIR spectrum observed by fixing the UV frequency to band C, which will be shown later.

Figure 3 shows three stable forms of fluorene−H_2O obtained by ab initio calculations at HF/6-31G and HF/6-31G(d,p) levels. Calculated energies and OH stretching frequencies are listed in Table 2. In the minimum energy conformer I, a water molecule locates above the middle of the fluorene molecule, and its hydrogen atoms are bound to two benzene rings through the π-type hydrogen bond. In conformer II, on the other hand, a water molecule is bound to one of the benzene rings. This structure is very similar to that of the benzene−H_2O cluster reported by Zwier et al.[34,35] In conformer III, the oxygen atom of H_2O is lying in the same plane of the aromatic ring, but at the opposite side of the hydrogen atoms of the central methylene group. In this configuration, the lone pair electrons of oxygen are interacting with the closely lying hydrogen atoms of the two benzene rings on both sides. It is seen from Table 2 that the relative energies of the conformers change at different calculation levels.

The simulated spectra for the three conformers at the HF/6-31G(d,p) level are presented in Figure 4, which are compared with the observed FDIR (Figure 4a) and FDSR (Figure 4a′) spectra. In Figure 4, stick diagrams (b)−(d) show the calculated IR spectra of the OH stretch bands for the conformers I−III, respectively. Similarly, the stick diagrams (b′)−(d′) show the calculated Raman spectra for the three conformers. As seen in the figure, the calculated OH stretching vibrational frequencies are more or less the same among the conformers. However, the relative band intensities of the simulated IR and Raman bands for conformers I and III show a better agreement with the observed spectra than those of conformer II. In conformer II, the calculated IR intensity of the symmetric mode is rather strong, which does not reproduce the observed one. Bernstein's group proposed that fluorene−H_2O may have the structure of conformer II from the L−J potential calculation.[39] The poor agreement between the observed and calculated IR spectra, however, suggests that conformer II may not be the probable conformer. As for conformers I and III, because both the calculated spectra reproduced well the observed IR and Raman spectra of the OH region, it is difficult to discriminate one of them only from the OH stretching vibrations.

To determine which conformer is the most probable one for fluorene−H_2O, we examined the CH stretching vibrations. As shown in Figure 3, the difference in intermolecular binding between fluorene and water is quite obvious; the water molecule of conformer III is lying in the same plane of the aromatic ring and its lone pair electron is interacting with the aromatic CH hydrogen. In conformer I, on the other hand, the water molecule is bound to the aromatic ring by a π-type hydrogen bond. In addition, it is seen that the lone pair electron of H_2O is interacting with the central methylene group. Thus, either the aromatic CH stretching or aliphatic CH stretching vibration may show a characteristic shift in the two conformers.

Figure 5 shows the calculated IR spectra of the CH stretching vibrations of (a) bare fluorene and (b)−(d) the fluorene site of the three fluorene−H_2O conformers. It is seen that a higher frequency aliphatic CH stretching vibration shows a large blue shift in conformer I compared to that of bare fluorene, while shifts of the aromatic CH stretching vibrations are very small in all the conformers. Figure 5e also shows the calculated spectrum of the aliphatic CH stretch vibration for fluorene−$(H_2O)_2$, which will be discussed later.

In Figure 6 are shown the FDIR spectra of (a) fluorene and (b),(c) fluorene−$(H_2O)_{1,2}$ in the aliphatic CH stretching region. In Figure 6b, the highest frequency aliphatic CH stretching band of fluorene−H_2O is blue shifted as large as 6 cm^{-1} compared to bare fluorene, while shifts of other vibrations are very small. This behavior is well reproduced in the calculated spectrum of

TABLE 2: Energies and Frequencies of the OH Stretching Vibrations for Fluorene−Water Clusters Obtained at the HF/6-31G and HF/6-31G(d,p) Level Calculations

	conformer I		conformer II		conformer III		assignments[a]
	HF/6-31G	HF/6-31G(d,p)	HF/6-31G	HF/6-31G(d,p)	HF/6-31G	HF/6-31G(d,p	
			Fluorene−H_2O				
ΔE^b	0	0	140	159	85	84	
	3611(4)	3622(20)	3617(10)	3624(39)	3612(10)	3622(27)	ν_1
	3746[c](43[d])	3718(45)	3750(11)	3719(37)	3751(69)	3725(70)	ν_3
			Fluorene−$(H_2O)_2$				
ΔE^b	0	0	2595	1731			
	3494(252)	3554(168)	3610(10	3621(18)			ν_1
	3609(38)	3610(64)	3614(4)	3623(19)			ν_1
	3718(81)	3696(94)	3747(70)	3717(38)			ν_3
	3740(93)	3699(55)	3748(50)	3719(53)			ν_3

[a] ν_3, antisymmetric OH stretching mode; ν_1, symmetric OH stretching mode. [b] ΔE is the difference in energy in cm^{-1} with respect to the minimum energy conformer. [c] Calculated frequencies are multiplied by a factor of 0.906 at the HF/6-31G level and 0.874 at the HF/6-31G(d,p) level. [d] IR intensity (km/mol) are presented in parentheses for calculated frequencies.

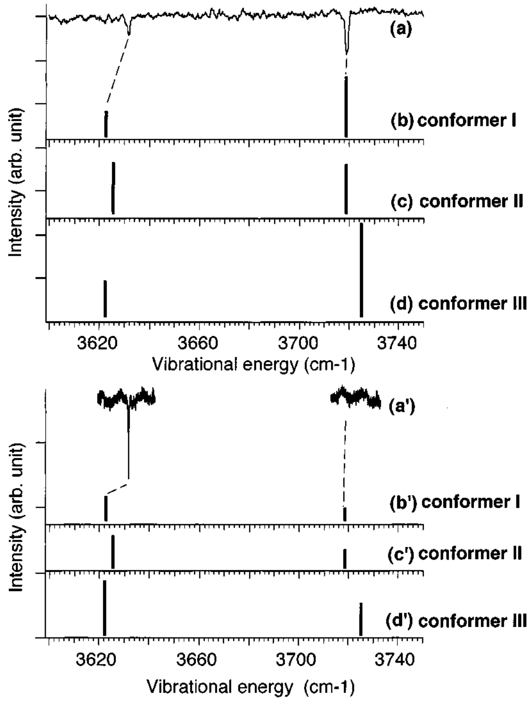

Figure 4. (a) FDIR and (a′) FDSR spectra of the OH stretching vibration of fluorene−H_2O. (b)−(d) Simulated IR spectra for conformers I−III at the HF/6-31G(d,p) level calculation, respectively. (b′)−(d′) simulated Raman spectra for conformers I−III at the HF/6-31G(d,p) level calculation.

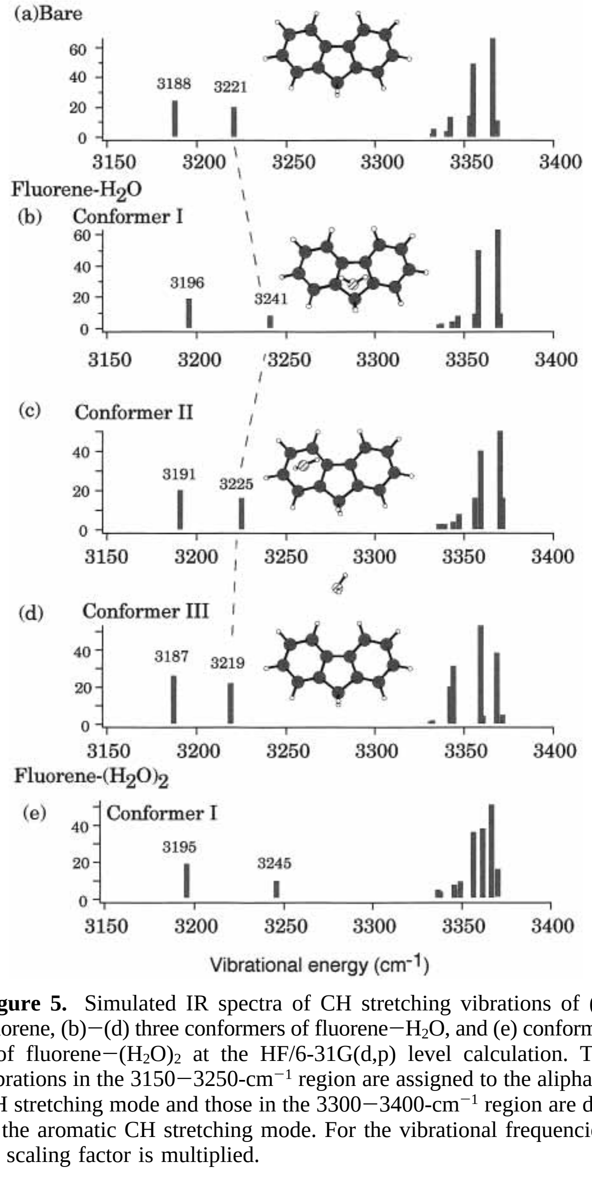

Figure 5. Simulated IR spectra of CH stretching vibrations of (a) fluorene, (b)−(d) three conformers of fluorene−H_2O, and (e) conformer I of fluorene−$(H_2O)_2$ at the HF/6-31G(d,p) level calculation. The vibrations in the 3150−3250-cm^{-1} region are assigned to the aliphatic CH stretching mode and those in the 3300−3400-cm^{-1} region are due to the aromatic CH stretching mode. For the vibrational frequencies, no scaling factor is multiplied.

conformer I (Figure 5b). Thus, the comparison between the observed and the calculated CH vibrations strongly supports the most probable form of fluorene−H_2O to be conformer I. The reason for the blue shift of aliphatic CH stretch is thought to be due to the deformation of the central methylene group owing to the interaction of methylene hydrogen and the lone pair electron of H_2O. Table 3 shows the calculated CH bond lengths and HCH bond angle of the central methylene group of fluorene and fluorene−H_2O. As seen in the table, the HCH bond angle increases and the CH bond length becomes shorter for conformer I, while changes in the other conformer are very small.

It should be noted that the aliphatic CH stretch shows further blue shift in fluorene−$(H_2O)_2$ (Figure 6c). This blue shift suggests that one of the water molecules in fluorene−$(H_2O)_2$ also has a similar conformation to that of fluorene−H_2O.

2. Fluorene−$(H_2O)_2$. As shown in Figure 1b, the origin for fluorene−$(H_2O)_2$ (band C) occurs at the 42 cm^{-1} higher frequency side from the origin of the fluorene monomer. Figure 7a,b shows the FDIR and FDSR spectra for fluorene−$(H_2O)_2$ obtained by fixing the UV frequency to band C in Figure 1b. All the observed frequencies are listed in Table 1. In the FDIR spectrum, four OH stretching bands are identified at 3527, 3604, 3706, and 3722 cm^{-1}, corresponding to four OH oscillators of two water molecules. The unusual structure of the 3710 cm^{-1}

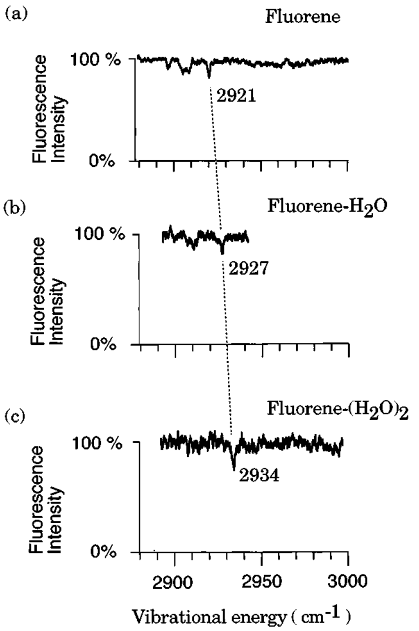

Figure 6. FDIR spectra of the aliphatic CH stretching vibrations of (a) fluorene and (b),(c) fluorene−$(H_2O)_{1,2}$.

TABLE 3: Calculated HCH Bond Angle and CH Bond Lengths of the Central Methylene of Fluorene and Three Conformers of Fluorene−H_2O

	H_1CH_2 angle (deg)	CH bond lengths(A)	
		CH_1[a]	CH_2
fluorene	107.25	1.0873	1.0873
fluorene−H_2O			
conformer I	107.85	1.0855	1.0871
conformer II	107.33	1.0870	1.0871
conformer III	107.20	1.0874	1.0883

[a] CH group, which is bound to H_2O.

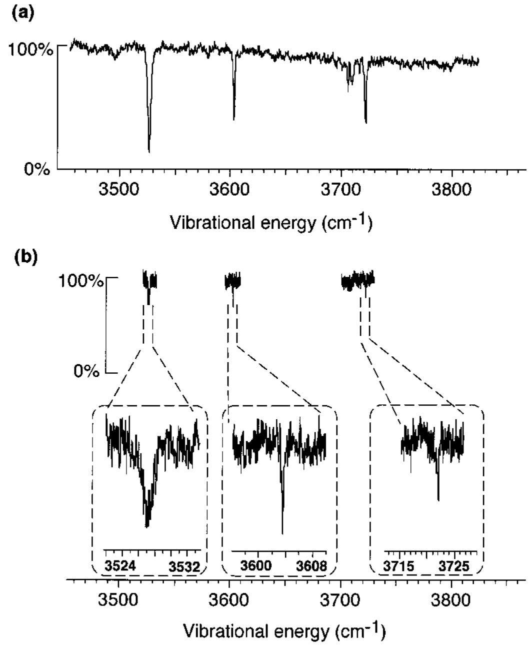

Figure 7. (a) FDIR and (b) FDSR spectra of fluorene−$(H_2O)_2$ obtained by monitoring band C of Figure 1.

band is due to the water vapor absorption of the IR intensity. In both the spectra, the intensity alternation between IR and Raman bands is not evident, indicating that four OH oscillators of two waters are not equivalent in the cluster.

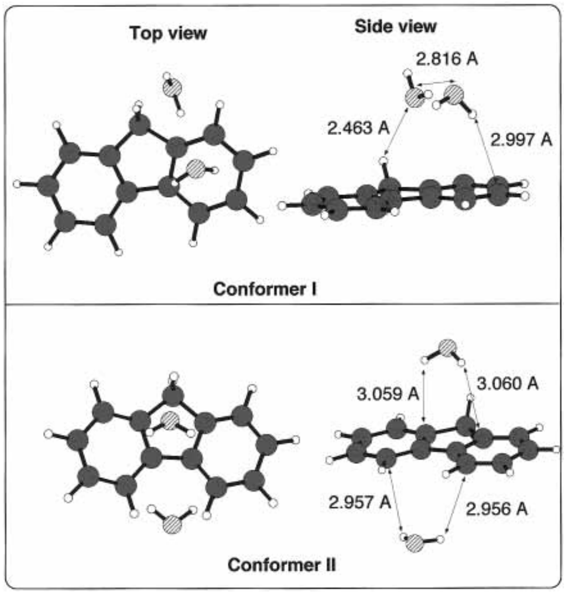

Figure 8. Energy-optimized structures at the HF/6-31G(d,p) level calculation. Structures are presented at two visual angles.

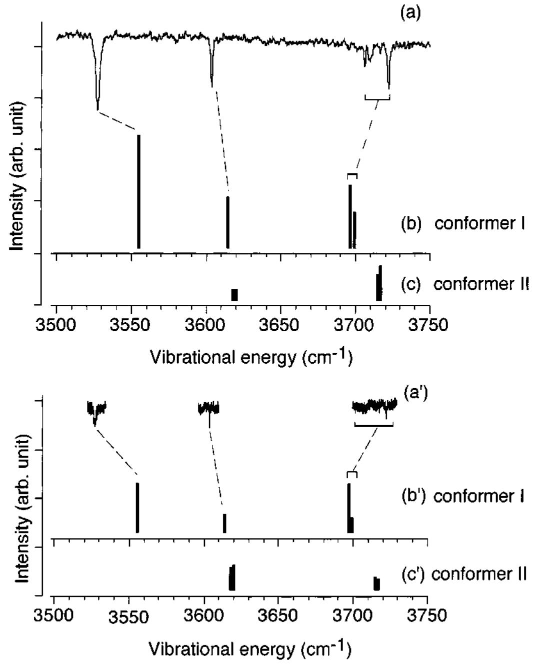

Figure 9. (a) FDIR and (a′) FDSR spectra of fluorene−$(H_2O)_2$. (b) and (c) are the simulated IR spectra for conformers I and II at the HF/6-31G(d,p) level calculation. (b′) and (c′) are the simulated Raman spectra for conformers I and II.

Figure 8 shows the ab initio calculated equilibrium structures for fluorene−$(H_2O)_2$. Calculated energies and frequencies are listed in Table 2. Conformer I is the minimum energy form in which a water dimer, $(H_2O)_2$, is located above the fluorene plane. In this conformer, a hydrogen of one water is bound to one of the benzene rings through a π-type hydrogen bond, and the lone pair electron of the other water is bound to a hydrogen of the central methylene of fluorene. On the other hand, conformer II is a very high energy conformer in which each water molecule locates at opposite sides of the fluorene plane.

Figure 9 represents comparisons of the FDIR and FDSR spectra with the simulated spectra obtained by the HF/6-31G-(d,p) level calculation for the two conformers. It is seen that the band positions and the relative intensities of the calculated

OH vibrations for conformer I show better agreement with those of the observed bands than those of conformer II. From the vector diagrams of the corresponding band, we assigned the 3722- and 3706-cm^{-1} bands of fluorene$-(H_2O)_2$ to the acceptor antisymmetric and donor free OH vibrations, respectively.[43] The 3604-cm^{-1} band corresponds to the π-type hydrogen-bonded OH stretching vibration, while the band at 3527 cm^{-1} corresponds to the σ-hydrogen-bonded OH stretching vibration. For the higher energy conformer II, either the position or relative intensities of simulated OH modes does not agree with the observed FDIR and FDSR spectra. In addition, the observed blue shift of the aliphatic CH stretching vibration in Figure 6c is also well reproduced in the calculated spectrum of conformer I in Figure 5e. Therefore, from the experimental and calculated results we conclude that the lowest energy conformer I is the probable structure for the fluorene$-(H_2O)_2$ cluster.

Conclusions

In this paper, we have presented the IR−UV and stimulated Raman−UV double-resonance spectroscopic studies of the fluorene$-(H_2O)_{n=1 \text{ and } 2}$ clusters. The alternation of intensities of the OH stretching modes in the IR and stimulated Raman spectra allow us to assign properly the symmetric and antisymmetric modes of the water site. The hydrogen-bonded OH stretching modes are distinguished from their red shifts. The stable structures and their OH and CH stretching vibrations were simulated at Hartree−Fock level molecular orbital calculations, which were used to determine the probable cluster structure. Not only the OH stretching vibration but also the CH stretching vibration of fluorene showed characteristic shifts, which were very useful in determining the most probable structure of the fluorene$-H_2O$ cluster. For fluorene$-(H_2O)_2$, its structure is the one in which a water dimer locates above the fluorene plane and is bound to the benzene π-plane and aliphatic CH group by weak hydrogen-bonds.

Acknowledgment. N.G. would like to acknowledge JSPS for providing the fellowship. N.G. also wishes to thanks his lab mates for their kind help (especially Drs. A. Fujii, T. Watanabe, and Y. Matsuda and Mr. Y. Matsumoto, R. Yamamoto, and A. Okazaki). This work is partially supported by the Grant-in-Aids for Scientific Research (10440165) by the Ministry of Education, Science, Sports and Culture, Japan.

References and Notes

(1) Vermon, M. F.; Krajnovich, D. J.; Kwok, H. S.; Lisy, J. M.; Shen, Y. R.; Lee, Y. T. *J. Chem. Phys.* **1982**, *77*, 47.

(2) Kim, K. S.; Mhin, B. J.; Lee, S. J.; Kim, K. S. *Chem. Phys. Lett.* **1994**, *219*, 243.

(3) Liu, K.; Gregory, J. K.; Brown, M. J.; Carter, C.; Saykally, R. J.; Clary, D. C. *Nature* (London) **1996**, *381*, 501.

(4) Liu, K.; Brown, M. G.; Saykally, R. J. *J. Phys. Chem. A* **1997**, *101*, 8995, and references therein.

(5) Buck, U.; Ettischer, I.; Melzer, M.; Buch, V.; Sadlej, J. *Phys. Rev. Lett.* **1998**, *80*, 2578.

(6) Pedulla, J. M.; Jordan, K. D. *Chem. Phys.* **1998**, *239*, 593.

(7) Ito, M.; Ebata., T.; Mikami, N. *Annu. Rev. Phy. Chem.* **1988**, *39*, 123.

(8) Felker, P. M.; Maxton, P. M.; Schaeffer, M. W. *Chem. Rev.* **1994**, *94*, 1787.

(9) Shang, Q. Y.; Bernstein, E. R. *Chem. Rev.* **1994**, *94*, 2015.

(10) Abe, H.; Mikami, N.; Ito, M. *J. Phys. Chem.* **1982**, *86*, 1768.

(11) Lipert, R. J.; Colson, S. D. *J. Phys. Chem.* **1990**, *94*, 2358.

(12) Roth, W.; Schmitt, M.; Jacoby, Ch.; Spangenberg, D.; Janzen, Ch.; Kleinermans, K. *Chem. Phys.* **1998**, *239*, 1, and references therein.

(13) Palmer, P. M.; Topp, M. R. *Chem. Phys.* **1998**, *239*, 65.

(14) Gutowsky, H. S.; Emilsson, T.; Arunan, E. *J. Chem. Phys.* **1993**, *99*, 4883.

(15) Zwart, E.; Ter Meulen, J. J.; Meerts, W. L.; Coudert, L. H. *J. Mol. Spectrosc.* **1991**, *147*, 27.

(16) Tanabe, S.; Fujii, M.; Ebata, T.; Mikami. N. *Chem. Phys. Lett.* **1993**, *215*, 347.

(17) Watanabe, T.; Ebata, T.; Tanabe, S.; Mikami, N. *J. Chem. Phys.* **1996**, *105*, 408.

(18) Mitsuzuka, A.; Fujii, A.; Ebata, T.; Mikami, N. *J. Chem. Phys.* **1996**, *105*, 2618.

(19) Matsumoto, Y.; Ebata, T.; Mikami, N. *J. Chem. Phys.* **1998**, *109*, 6303.

(20) Matsuda Y.; Ebata, T.; Mikami, N. *J. Chem. Phys.* **1999**, *110*, 8397.

(21) Guchhait, N.; Ebata, T.; Mikami, N. *J. Chem. Phys.* **1999**, *111*, 8438.

(22) Fredericks, S. Y.; Jordan, K. D.; Zwier, T. S. *J. Phys. Chem.* **1996**, *100*, 7810.

(23) Hagemeister, F. C.; Gruenloh, C. J.; Zwier, T. S. *Chem. Phys.* **1998**, *239*, 83.

(24) Barth, H.-D.; Buchhold, K.; Djafari, S.; Reimann, B.; Lommatzsch, U.; Brutschy, B. *Chem. Phys.* **1998**, *239*, 49.

(25) Tarakeshwar, P.; Kim, K. S.; Brutschy, B. *J. Chem. Phys.* **1999**, *110*, 8501.

(26) Janzen, Ch.; Spangenberg, D.; Roth, W.; Kleinermanns, K. *J. Chem. Phys.* **1999**, *110*, 9898.

(27) Hartland, G. V.; Henson, B. F.; Venturo, V. A.; Felker, P. M. *J. Phys. Chem.* **1992**, *96*, 1164.

(28) Ishikawa, S.; Ebata, T.; Mikami, N. *J. Chem. Phys.* **1999**, *110*, 4238.

(29) Yamamoto, R.; Ishikawa, S.; Ebata, T.; Mikami, N. *J. Raman Spectrosc.* **2000**, 31, 295.

(30) Suzuki, S.; Green, P. G.; Bumgarner, R. E.; Dasgupta, S.; Goddard, W. A., III.; Blake, G. A. *Science* **1992**, *257*, 942.

(31) Helm, R. M.; Neusser, H. J. *Chem. Phys.* **1998**, *239*, 33.

(32) Berden, G.; Meerts, W. L.; Schmitt, M.; Kleinermanns, K. *J. Chem. Phys.* **1996**, *104*, 972.

(33) Ebata, T.; Furukawa, M.; Suzuki, T.; Ito, M. *Opt. Soc. Am. B* **1990**, *7*, 1890.

(34) Pribble, R. N.; Zwier, T. S. *Science* **1994**, *265*, 75.

(35) Pribble, R. N.; Zwier, T. S. *Faraday Discuss.* **1994**, *97*, 229.

(36) Tarakeshwar, P.; Kim, K. S.; Brutschy, B. *J. Chem. Phys.* **2000**, *112*, 1769.

(37) Helm, R. M.; Vogel, H.-P.; Neusser, H. J.; Storm, V.; Consalvo, D.; Dreizler, H. *Z. Naturforsch., A: Phys. Sci.* **1997**, *52*, 655.

(38) Donckt, E. V.; Nasielski, J.; Thiry, P. *Chem. Commun.* **1969**, 1289.

(39) Im, H. S.; Grassian, V. H.; Bernstein, E. R. *J. Phys. Chem.* **1990**, *94*, 222.

(40) Leutwyler, S.; Even, U.; Jortner, J. *J. Chem. Phys.* **1983**, *79*, 5769.

(41) Yip, W. T.; Levy, D. H.; Kobetic, R.; Piotrowiak, P. *J. Phys. Chem.* **1999**, *103*, 10.

(42) Herzberg G. *Molecular Spectra and Molecular Structure II. Infrared and Raman Spectra of Polyatomic Moleclues*; Van Nostrand Reinhold Co.: New York, 1945.

(43) Frisch, M. J.; Trucks, G. W.; Schlegel, H. B.; Gill, P. M. W.; Johnson, B. G.; Robb, M. A.; Cheeseman, J. R.; Keith, T.; Petersson, G. A.; Montgomery, J. A.; Raghavachari, K.; Al-Laham, M. A.; Zakrzewski, V. G.; Ortiz, J. V.; Foresman, J. B.; Cioslowski, J.; Stefanov, B. B.; Nanayakkara, A.; Challacombe, M.; Peng, C. Y.; Ayala, P. Y.; Chen, W.; Wong, M. W.; Andres, J. L.; Replogle, E. S.; Gomperts, R.; Martin, R. L.; Fox, D. J.; Binkley, J. S.; Defrees, D. J.; Baker, J.; Stewart, J. P.; Head-Gordon, M.; Gonzalez, C.; Pople, J. A. *Gaussian 94*, revision x.x; Gaussian, Inc.: Pittsburgh, PA, 1995.